Nonlinear force-free fields and coronal magnetic field modeling

M. S. Wheatland

Sydney Institute for Astronomy
School of Physics
The University of Sydney

NCAR/HAO Colloquium
19 October 2016, NCAR Center Green
Boulder CO

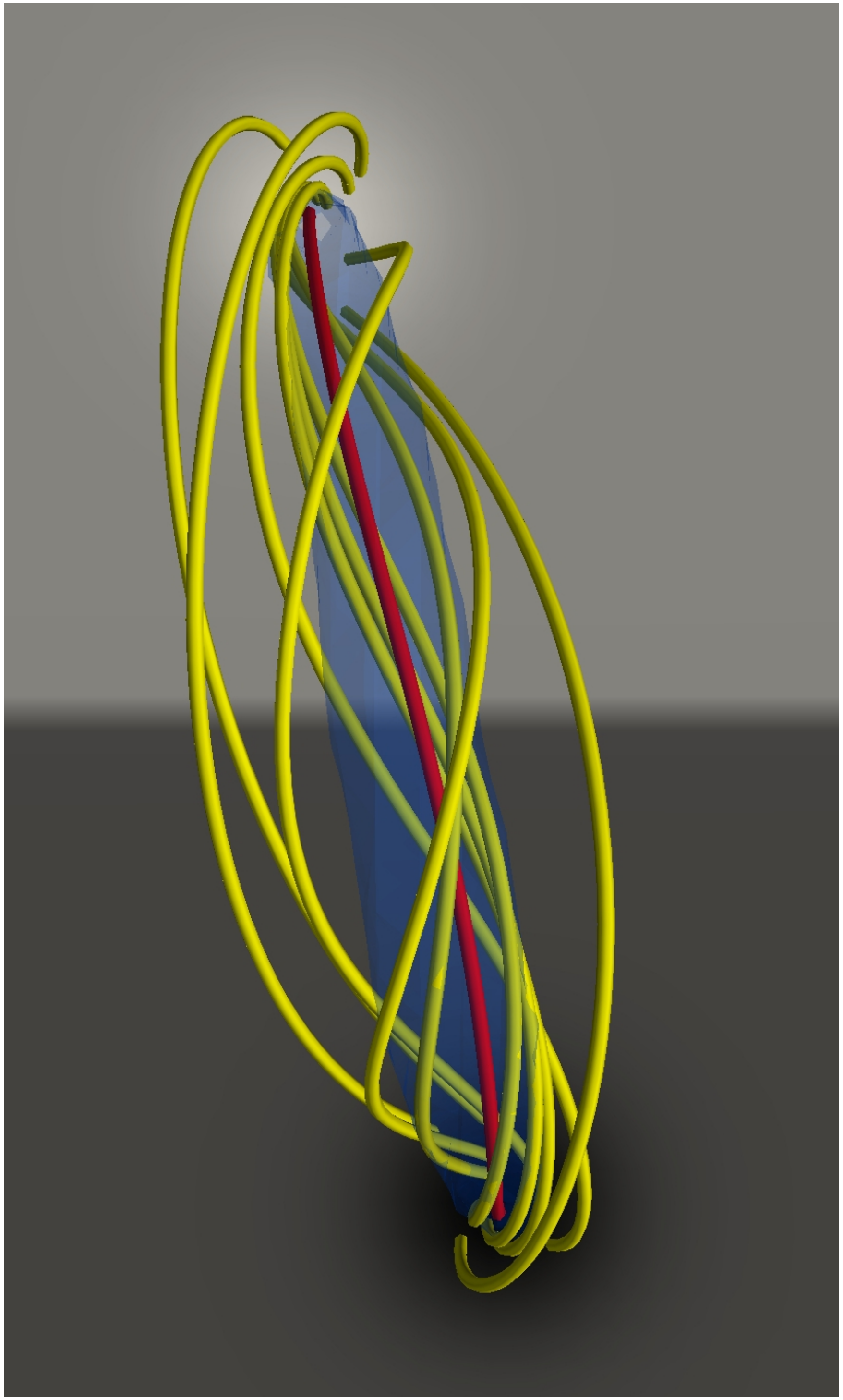

Overview

Background

- *Motivation for coronal magnetic field modeling*
- *The popularity of the nonlinear force-free field (NLFFF) model*

NLFFF modeling

- *Vector magnetogram data*
- *The model and the boundary conditions*
- *The cfit code*
- *Results for analytic bipole BCs*
- *Whence the maximum energy?*
- *Which is the minimum energy?*

Summary

Background: Motivation for coronal magnetic field modeling

- Sunspot magnetic fields power large-scale solar activity
  - solar flares, coronal mass ejections
- Solar activity motivates coronal magnetic field modeling
  - to understand and quantify magnetic energy release
  - to improve flare and space weather prediction
- The Nonlinear Force-Free Field (NLFFF) model is popular
  - a static model involving only the magnetic field $\boldsymbol{B}$
  - the 'simplest plausible model which includes free energy'
  - justifications: low plasma β, slow driving, large coronal v_A
    (cf. Peter et al. 2015)
  - the model presents a boundary value problem for $\boldsymbol{B}$ and α
    - where α is the force-free parameter
  - solar data (vector magnetograms) provide BCs

Background: The popularity of the NLFFF model

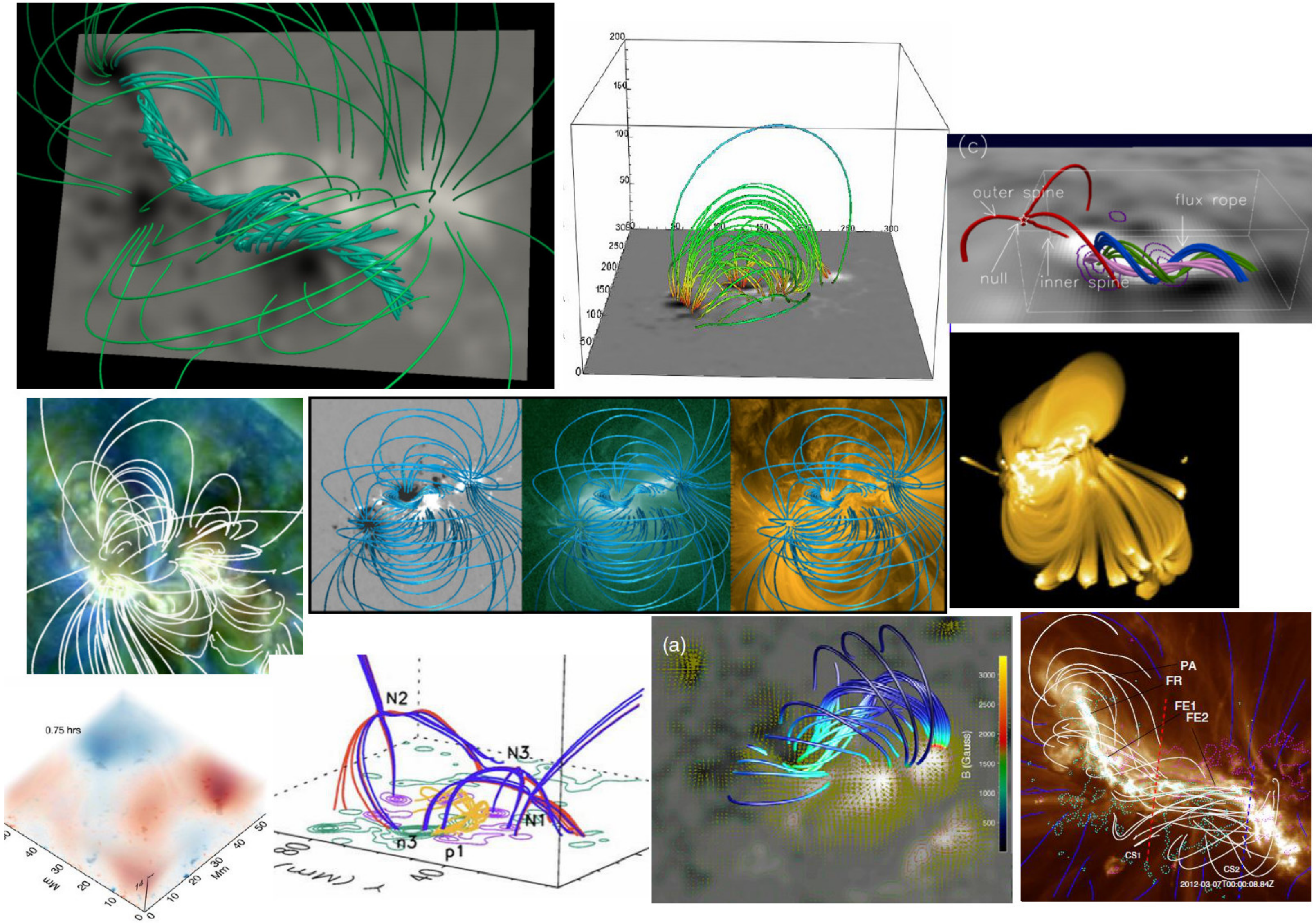

Top row L to R: Chintzoglou et al. (2015); Moraitis et al. (2014); Yang et al. (2015). Middle row: Tadesse et al. (2015); Inoue et al. (2014); Cheung et al. (2015). Bottom row: Chitta et al. (2014); Mandrini et al. (2014); Cheng et al. (2014); Wang et al. (2014).

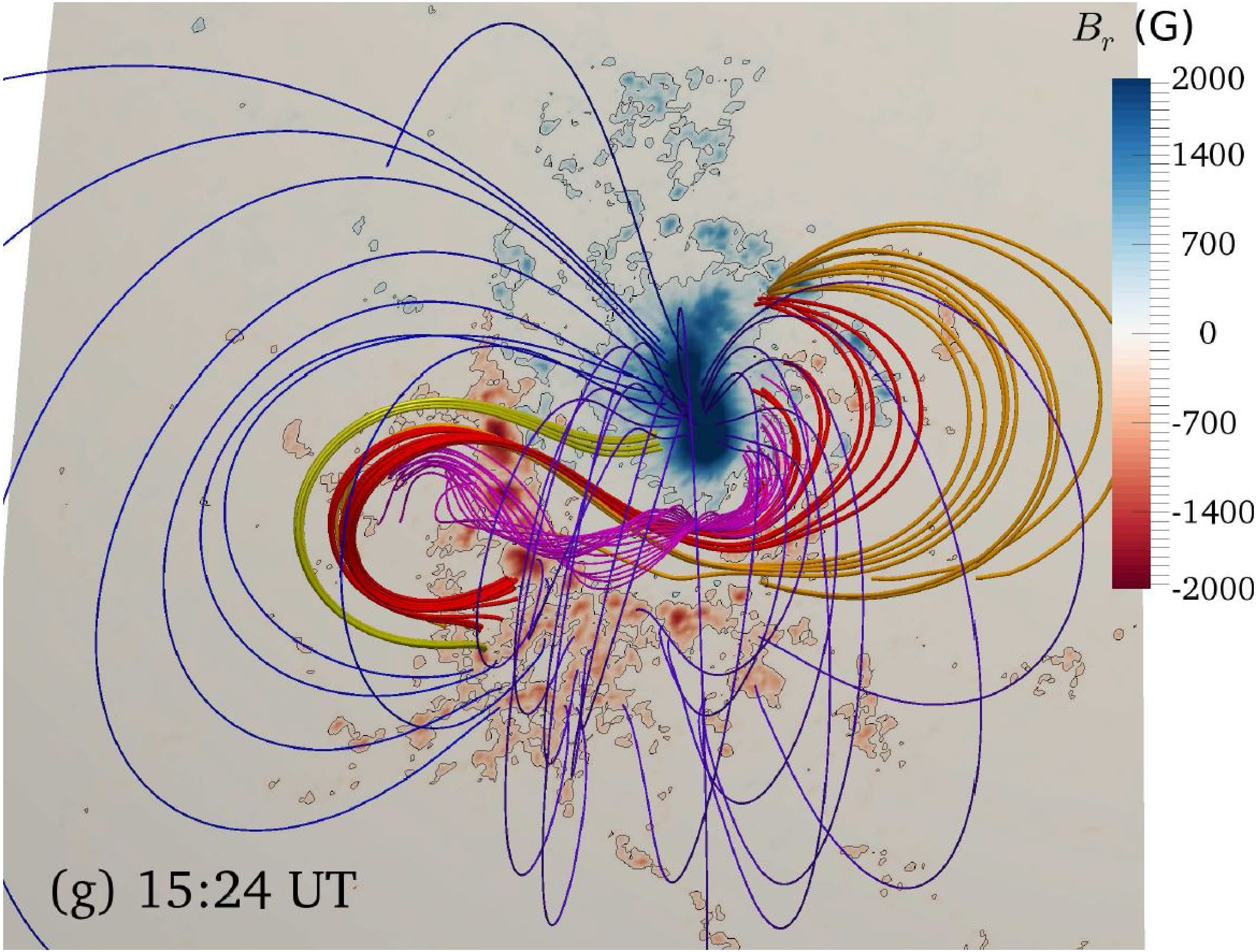

AR12158 on 10 September 2014 (Zhao et al. 2016; calculation: S.A. Gilchrist)

NLFFF modeling: Vector magnetogram data

Nobody can measure physical quantities of the solar atmosphere
(del Toro Iniesta & Ruiz Cobo 1996)

- Photospheric lines reveal $\boldsymbol{B}$ via the Zeeman effect
  (del Toro Iniesta 2003)
  - Stokes inversion: the process of inferring values for $\boldsymbol{B}$
    - from the measured polarisation state of the line
  - an inference rather than a direct measurement
- the 180 degree ambiguity in $B_\perp$ must also be resolved
  (Metcalf 1994; Metcalf et al. 2006; Leka et al. 2009)
- Vector magnetogram: photospheric map of $\boldsymbol{B} = (B_x, B_y, B_z)$
  - local heliocentric co-ordinates (z is local radial direction)
- Space-based instruments: Hinode/SOT-SP, SDO/HMI
  (Tsuneta et al. 2008; Schou et al. 2012)
  - the data provide BCs for NLFFF modeling

NLFFF modeling: The model

- Force-free model for a magnetic field $\boldsymbol{B}$:
  (Wiegelmann & Sakurai 2012)

$$\boldsymbol{J} \times \boldsymbol{B} = 0 \quad \text{and} \quad \operatorname{div} \boldsymbol{B} = 0 \tag{1}$$

  - where $\boldsymbol{J} = \mu_0^{-1} \nabla \times \boldsymbol{B}$ is the current density
- We have $\boldsymbol{J}$ parallel to $\boldsymbol{B}$ so writing $\boldsymbol{J} = \alpha \boldsymbol{B} / \mu_0$:

$$\nabla \times \boldsymbol{B} = \alpha \boldsymbol{B} \tag{2}$$

  - where α is the force-free parameter
- Taking the divergence of Eq. (2) gives

$$\boldsymbol{B} \cdot \nabla \alpha = 0 \tag{3}$$

  - using $\operatorname{div} \boldsymbol{B} = 0$
- Eqs. (2) and (3) are equivalent to Eqs. (1)
  - four coupled nonlinear PDEs for dependent variables $(\boldsymbol{B}, \alpha)$

NLFFF modeling: The boundary conditions

- Boundary conditions in a half space: (Grad & Rubin 1958)
  - B_z at $z = 0$
  - α at $z = 0$ over one polarity of B_z
    - because $\boldsymbol{B} \cdot \nabla\alpha = 0 \Rightarrow \alpha$ is constant along $\boldsymbol{B}$
    - the choices of polarity are labelled P ($B_z > 0$) and N ($B_z < 0$)
- Vector magnetograms provide BCs over both polarities using

$$\alpha|_{z=0} = \frac{1}{B_z}\left(\frac{\partial B_y}{\partial x} - \frac{\partial B_x}{\partial y}\right)\Big|_{z=0} \quad (4)$$

  - so in principle two solutions: the "P and N solutions"

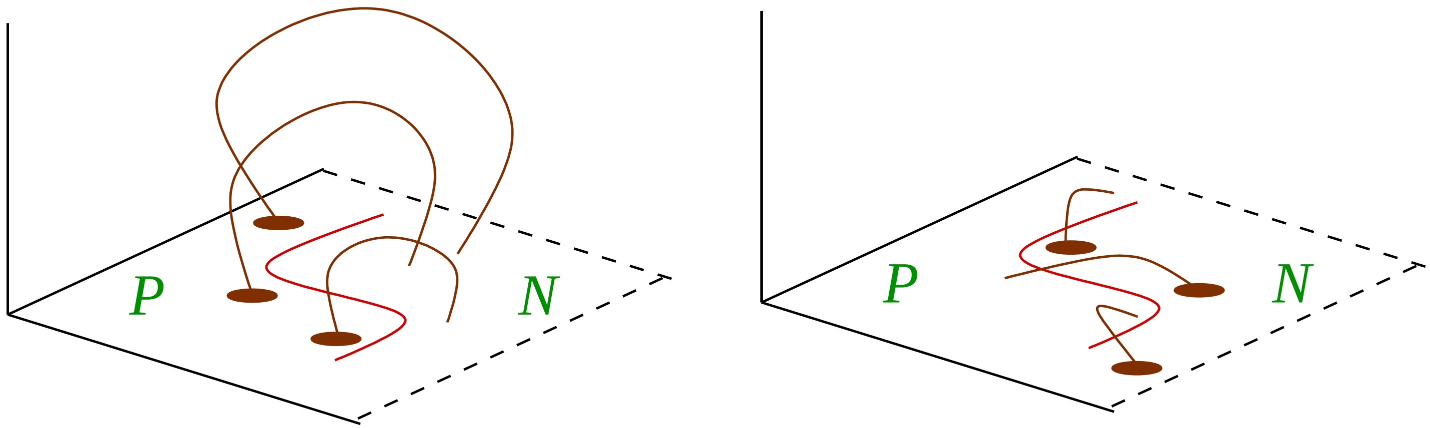

P solution *N* solution

NLFFF modeling: The cfit code

- cfit: cartesian current-field iteration (Grad-Rubin) code (Wheatland 2007)
  - Grad-Rubin iteration involves two steps at each iteration k: (Grad & Rubin 1958)

$$\text{Current update:} \qquad \boldsymbol{B}^{[k-1]} \cdot \nabla \alpha^{[k]} = 0 \tag{5}$$

$$\text{Field update:} \qquad \nabla \times \boldsymbol{B}^{[k]} = \alpha^{[k]} \boldsymbol{B}^{[k-1]} \tag{6}$$

    - a fixed point provides a solution to the NLFFF equations
  - the solution volume V is $0 \leq x \leq L_x$, $0 \leq y \leq L_y$, $0 \leq z \leq L_z$
  - the BCs are the specification at each iteration of

$$B_z^{[k]}\Big|_{z=0} \quad \text{and} \quad \alpha^{[k]}(x,y,0)\Big|_P \quad \text{or} \quad \alpha^{[k]}(x,y,0)\Big|_N \tag{7}$$

    - as well as $B_z^{[k]}\Big|_{z=L_z} = 0$
    - and periodicity of the fields in x and y
  - Eq. (5) is solved using field-line tracing
  - Eq. (6) is solved using 2-D FFTs
  - the iteration sequence starts with the potential field $\boldsymbol{B}^{[0]} = \boldsymbol{B}_0$

NLFFF modeling: The cfit code

- The code uses the (Helmholtz) decomposition of the field:

$$\boldsymbol{B}^{[k]} = \boldsymbol{B}_0 + \boldsymbol{B}_{\rm c}^{[k]} \tag{8}$$

  - where $\boldsymbol{B}_0 = -\nabla\phi_0$ with boundary conditions:
    - $\hat{\boldsymbol{z}} \cdot \boldsymbol{B}_0$ matches $\hat{\boldsymbol{z}} \cdot \boldsymbol{B}^{[k]}$ on $z = 0$ and $z = L_z$
    - $\boldsymbol{B}_0$ is periodic in x and y
  - and $\boldsymbol{B}_{\rm c}^{[k]} = \nabla \times \boldsymbol{A}_{\rm c}^{[k]}$ with boundary conditions:
    - $\hat{\boldsymbol{z}} \cdot \boldsymbol{B}_{\rm c}^{[k]} = 0$ on $z = 0$ and $z = L_z$
    - $\boldsymbol{B}_{\rm c}^{[k]}$ is periodic in x and y
- The code solves $\nabla^2\phi_0 = 0$ and $\nabla^2 \boldsymbol{A}_{\rm c}^{[k]} = -\alpha^{[k]}\boldsymbol{B}^{[k-1]}$
- Eq. (8) and the BCs imply

$$\begin{aligned} E = \frac{1}{2\mu_0}\int_V |\boldsymbol{B}^{[k]}|^2 dV &= \frac{1}{2\mu_0}\int_V |\boldsymbol{B}_0 + \boldsymbol{B}_{\rm c}^{[k]}|^2 dV \\ &= \frac{1}{2\mu_0}\int_V |\boldsymbol{B}_0|^2 + |\boldsymbol{B}_c^{[k]}|^2 dV = E_0 + E_{\rm c}^{[k]} \end{aligned} \tag{9}$$

  - so E_0 is the minimum energy field for the specified BCs

NLFFF modeling: Results for analytic bipole BCs

- BCs for B_z:
  - two Gaussian spots
- BCs for α (P BCs):
  - a small patch $\alpha = \alpha_0 =$ const at the positive pole

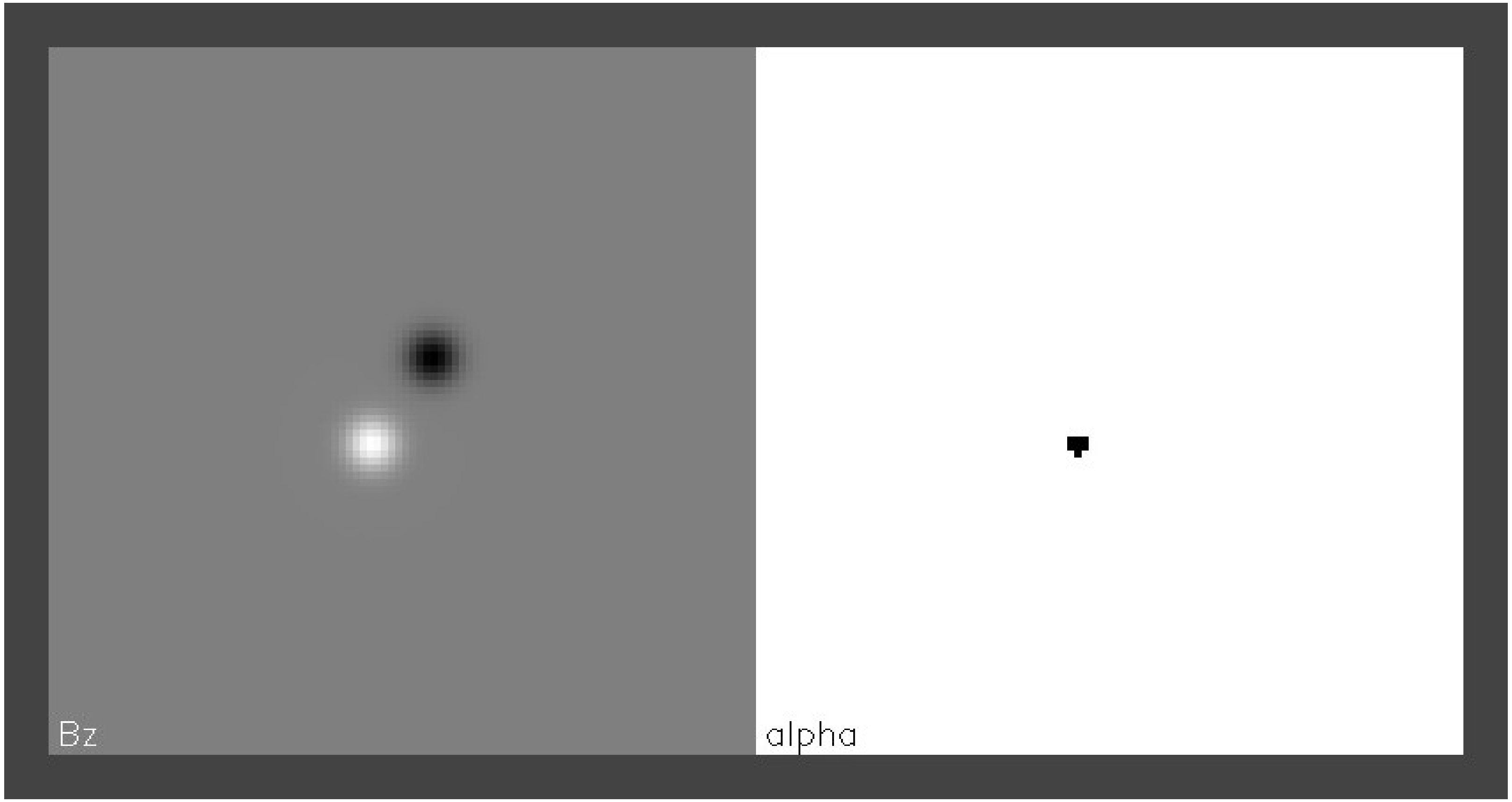

BCs for B_z (left) and α (right). The α values are shown in inverse.

NLFFF modeling: Results for analytic bipole BCs

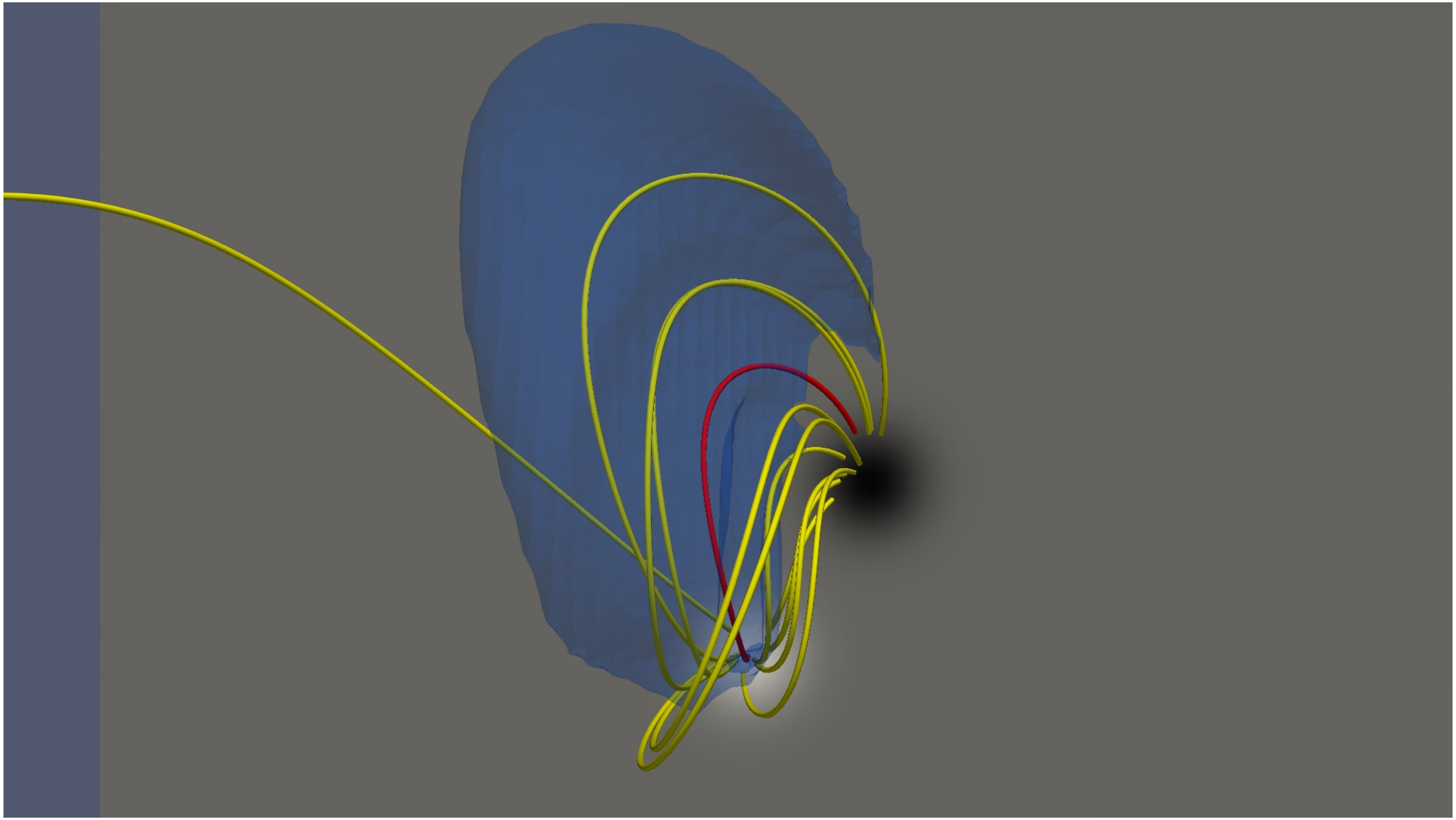

The end point of the Grad-Rubin iteration procedure with cfit.

NLFFF modeling: Results for analytic bipole BCs

- BCs for B_z:
  - two Gaussian spots
    - with a uniform background bipole field
- BCs for α (P BCs):
  - a small patch $\alpha = \alpha_0 =$ const at the positive pole

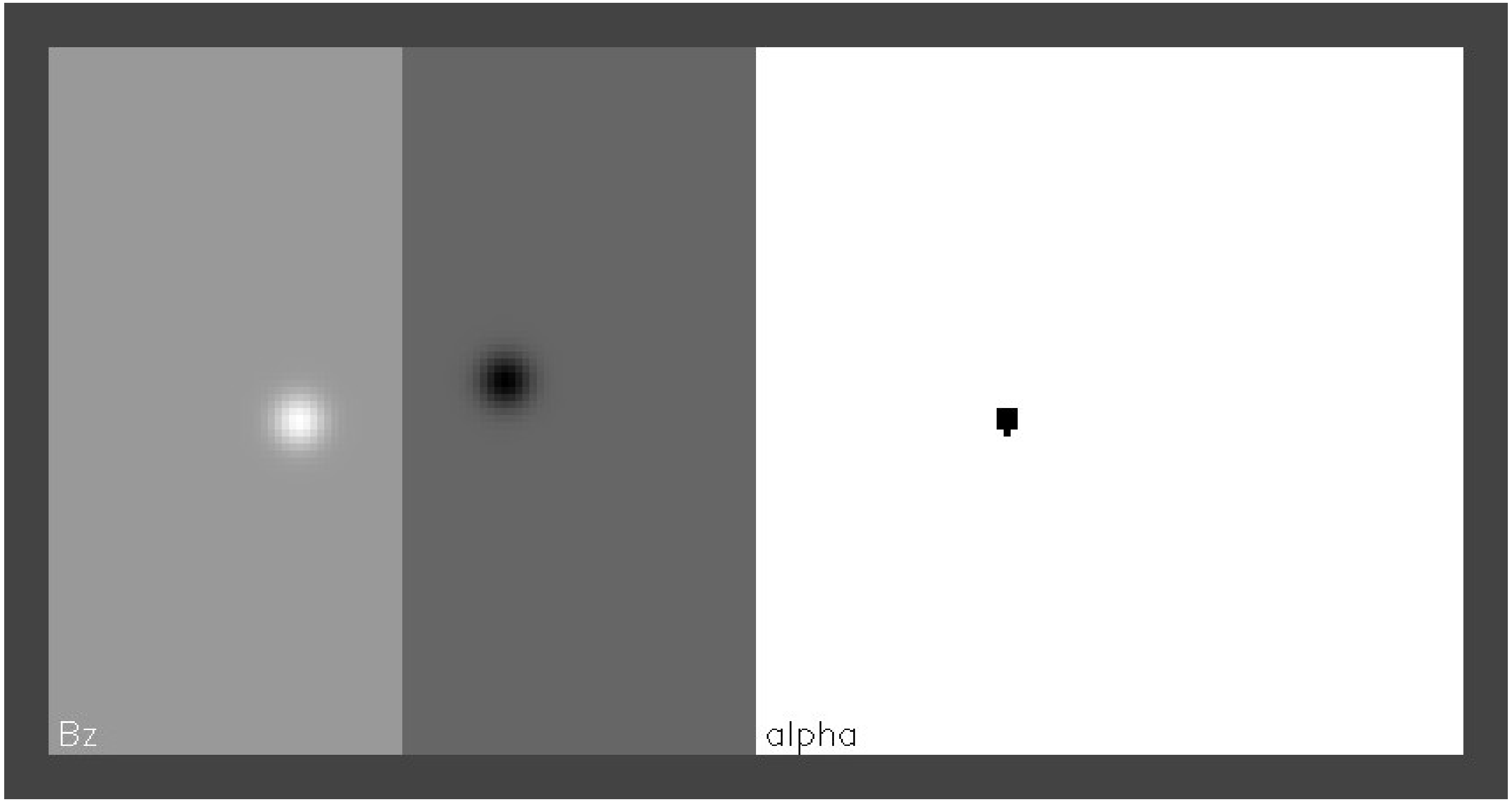

BCs for B_z (left) and α (right). The α values are shown in inverse.

NLFFF modeling: Results for analytic bipole BCs

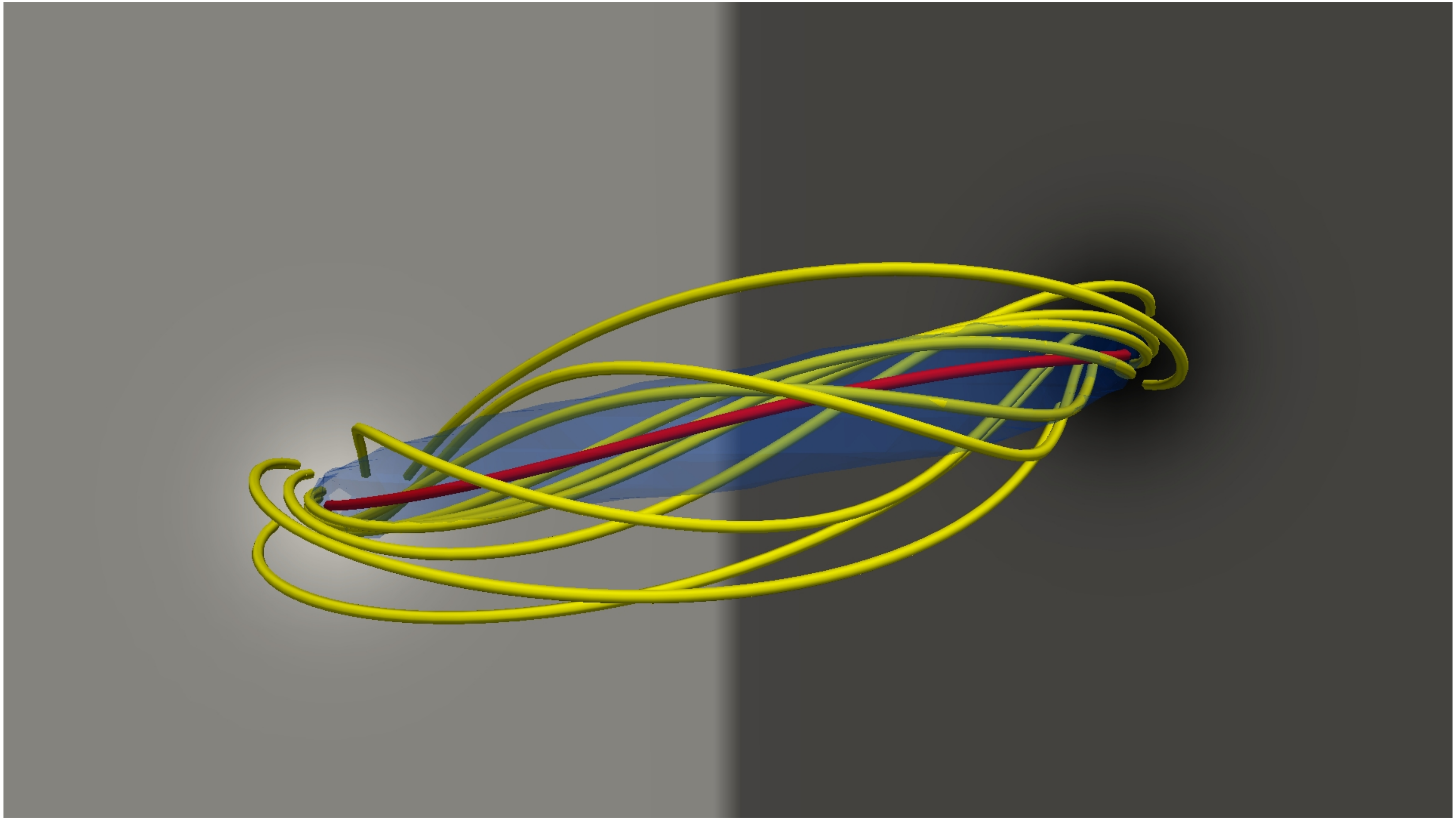

The end point of the Grad-Rubin iteration procedure with cfit.

NLFFF modeling: Results for analytic bipole BCs

- NLFFF solutions are obtained for a range of values of α_0
  - up to a maximum value $\alpha_{\max}$
  - for $\alpha_0 > \alpha_{\max}$ a fixed point is not obtained
- The solution energies scale as $E(\alpha_0) - E_0 \approx \text{const} \times \alpha_0^2$

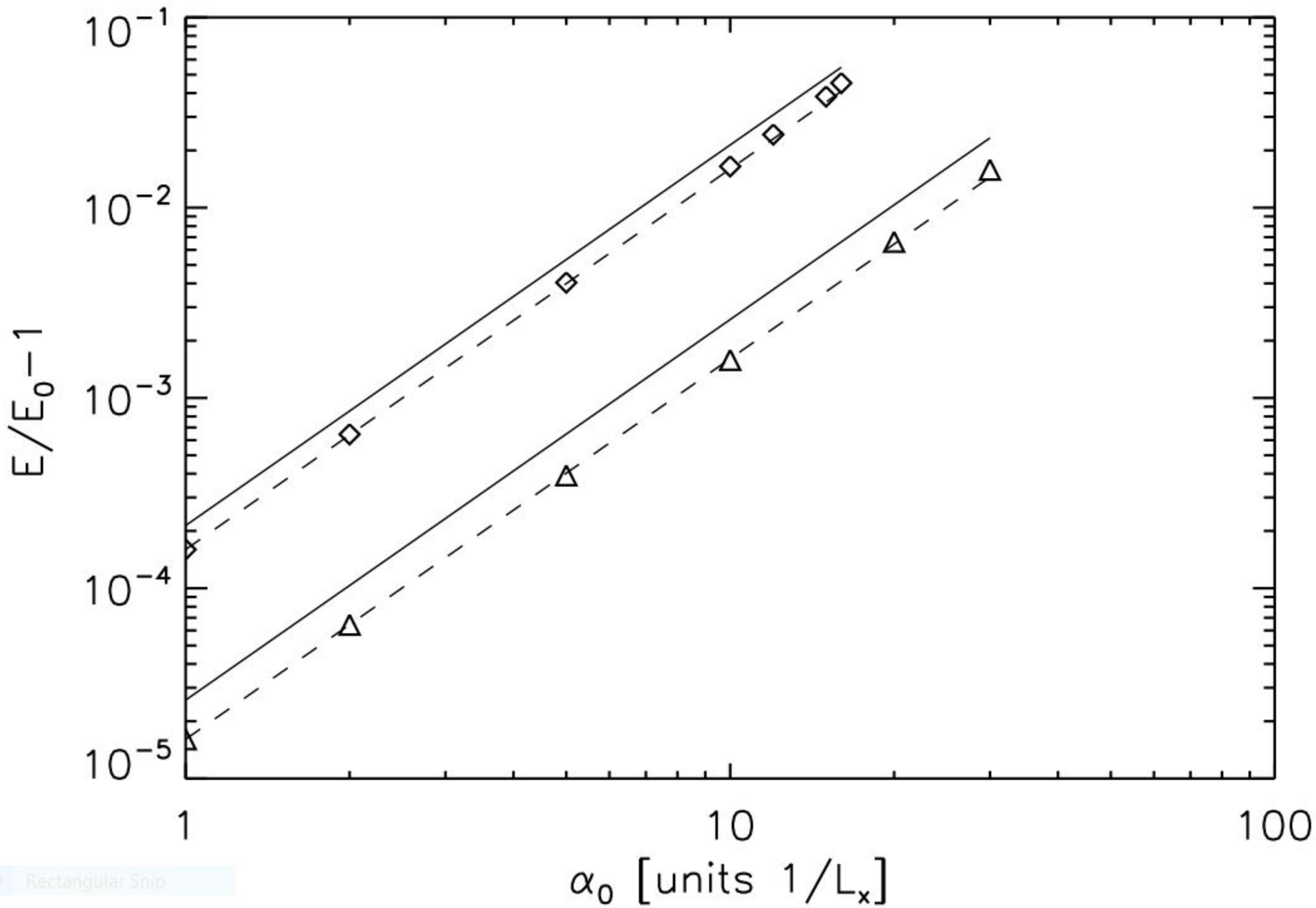

Log-log plot of $(E - E_0)/E_0$ versus α_0 for bipoles without (left) and with (right) a background field.

NLFFF modeling: Results for analytic bipole BCs

- The maximum 'free' energies are
  - $E/E_0 \approx 1.05$ (no background)
  - $E/E_0 \approx 1.02$ (with background)
    - note that E_0 is different in the two cases
- The scaling may be understood from the loop self-induction (e.g. Landau & Lifshitz 1960; Wheatland & Farvis 2003)
  - for a toroidal current loop with uniform current:

$$E_{\text{loop}} = \tfrac{1}{2} L i^2 \qquad (10)$$

$$\text{where} \quad L = \mu_0 a \left(\ln \frac{8a}{r} - \frac{7}{4} \right) \quad \text{and} \quad i = \alpha_0 \int_{z=0} B_z \, \mathrm{d}x \, \mathrm{d}y \qquad (11)$$

    - and where a is the major radius of the torus
    - and r is the minor radius
  - the solid lines in the figure indicate the E_{loop} values
  - for large α_0 (or i) we expect a departure due to $L = L(i)$
    - the current paths change as the loop twists, or distorts
    - longer paths imply larger inductance hence greater energy

NLFFF modeling: Whence the maximum energy?

- J.J. Aly identified an upper bound to the energy (Aly 1984)
  - in a half-space, for a specified B_z distribution
  - the derivation starts from the Virial theorem: (e.g. Low 1982)

$$\begin{aligned} \mu_0 E &= \int_{z=0} \boldsymbol{r} \cdot \boldsymbol{B} B_z \, \mathrm{d}x \, \mathrm{d}y \quad \text{where} \quad \boldsymbol{r} = (x, y) \\ &= \int_{z=0} r B_r \, B_z \, \mathrm{d}\sigma \le \left(\int_{z=0} (r B_z)^2 \, \mathrm{d}\sigma \int_{z=0} B_r^2 \, \mathrm{d}\sigma \right)^{1/2} \end{aligned} \tag{12}$$

    - using the Cauchy-Schwartz inequality with $\mathrm{d}\sigma = r \, \mathrm{d}r \, \mathrm{d}\phi$
  - and zero net force on the volume implies: (e.g. Molodenskii 1969)

$$\int_{z=0} B_r^2 \, \mathrm{d}\sigma = \int_{z=0} \left(B_x^2 + B_y^2 \right) \, \mathrm{d}\sigma = \int_{z=0} B_z^2 \, \mathrm{d}\sigma \tag{13}$$

  - so the bound in Eq. (12) is independent of B_x and B_y:

$$\begin{aligned} E \le E_{\mathrm{UB}} = \tfrac{1}{\mu_0} \left(I_1 I_2 \right)^{1/2} \\ \text{where} \quad I_1 = \int_{z=0} B_z^2 \, \mathrm{d}x \, \mathrm{d}y \quad \text{and} \quad I_2 = \int_{z=0} (x^2 + y^2) B_z^2 \, \mathrm{d}x \, \mathrm{d}y \end{aligned} \tag{14}$$

NLFFF modeling: Whence the maximum energy?

- The integral I_2 depends on the choice of origin
  - Aly identified this and said (Aly 1984)

    To get the best possible bound, we have to take the infinum... with respect to all possible Os

  - but assuming

$$I_2(x_0, y_0) = \int_{z=0} \left[(x - x_0)^2 + (y - y_0)^2\right] B_z^2 \,\mathrm{d}x \,\mathrm{d}y \qquad (15)$$

    - it is easy to show that the extremum E_{EUB} is achieved for

$$x_0 = \frac{1}{I_1} \int_{z=0} x\, B_z^2 \,\mathrm{d}x \,\mathrm{d}y \quad \text{and} \quad y_0 = \frac{1}{I_1} \int_{z=0} y\, B_z^2 \,\mathrm{d}x \,\mathrm{d}y \qquad (16)$$

    - i.e. the B_z^2-weighted average position
- For our bipole field B_z distributions $(x_0, y_0) = \frac{1}{2}(L_x, L_y)$ and:
  - $E_{\mathrm{EUB}}/E_0 \approx 4.3$ (no background)
  - $E_{\mathrm{EUB}}/E_0 \approx 5.9$ (with background)
  - and these are much larger than the NLFFF solution energies

NLFFF modeling: Whence the maximum energy?

- There is also the Aly-Sturrock limit: (Aly 1991; Sturrock 1991)
  - the "open field" energy E_{open} is the true upper bound?
  - but for our BCs (periodic in x and y)
    - excess flux at the lower boundary must exit the top
    - hence the open field has all field lines exiting the top
    - hence $B \to \text{const}$ as $z \to \infty$ so $E_{\text{open}} = \infty$

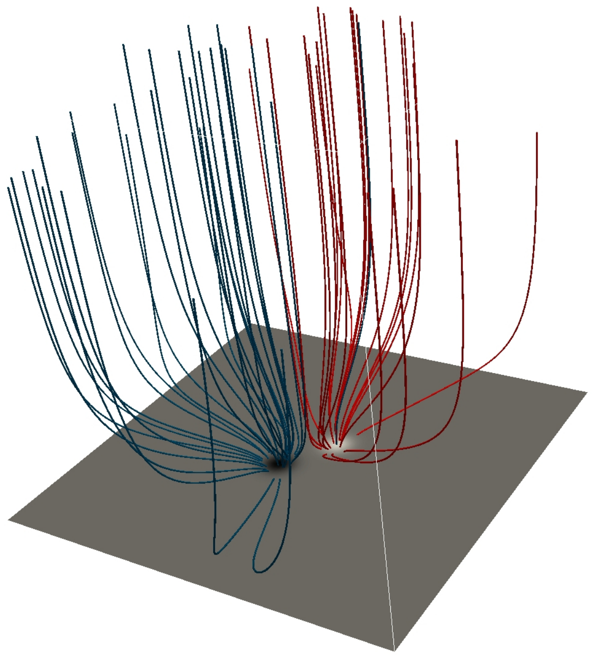

The Aly-Sturrock open field constructed for the bipole with no background.

- So we know that there is a "most energetic field"
  - but we don't know if cfit achieves that limit

NLFFF modeling: Which is the minimum energy?

- The usual field decomposition for the Thomson theorem is:
  (e.g. Jackson 1962; Valori et al. 2013)

$$\boldsymbol{B} = \boldsymbol{B}_{\rm P} + \boldsymbol{B}_{\rm J} \tag{17}$$

  - where $\boldsymbol{B}_{\rm P} = -\nabla\phi_{\rm P}$ with boundary conditions:
    - $\hat{\mathbf{n}} \cdot \boldsymbol{B}_{\rm P}$ matches $\hat{\mathbf{n}} \cdot \boldsymbol{B}$ on all boundaries
  - and $\boldsymbol{B}_{\rm J}$ is the non-potential component with BCs:
    - $\hat{\mathbf{n}} \cdot \boldsymbol{B}_{\rm J} = 0$ on all boundaries
- Eq. (17) and the BCs imply the Thomson/Dirichlet theorem:

$$\begin{aligned} E = \frac{1}{2\mu_0}\int_V |\boldsymbol{B}|^2 dV &= \frac{1}{2\mu_0}\int_V |\boldsymbol{B}_{\rm P} + \boldsymbol{B}_{\rm J}|^2 dV \\ &= \frac{1}{2\mu_0}\int_V |\boldsymbol{B}_{\rm P}|^2 + |\boldsymbol{B}_{\rm J}|^2 dV = E_{\rm P} + E_{\rm J} \end{aligned} \tag{18}$$

  - so $E_{\rm P}$ is the minimum energy field for the specified BCs

NLFFF modeling: Which is the minimum energy?

- **Question:** If this decomposition is applied to cfit results (e.g. Valori et al. 2013; De Rosa et al. 2015)
  - then we have both field decompositions:

$$\begin{aligned} \boldsymbol{B} &= \boldsymbol{B}_0 + \boldsymbol{B}_\mathrm{c} \\ &= \boldsymbol{B}_\mathrm{P} + \boldsymbol{B}_\mathrm{J} \end{aligned} \tag{19}$$

  - which is the minimum energy, E_0 or E_P?

NLFFF modeling: Which is the minimum energy?

- **Question:** If this decomposition is applied to cfit results
  (e.g. Valori et al. 2013; De Rosa et al. 2015)
  - then we have both field decompositions:

$$\begin{aligned} \boldsymbol{B} &= \boldsymbol{B}_0 + \boldsymbol{B}_{\mathrm{c}} \\ &= \boldsymbol{B}_{\mathrm{P}} + \boldsymbol{B}_{\mathrm{J}} \end{aligned} \tag{20}$$

  - which is the minimum energy, E_0 or E_{P}?

- **Answer:** It can be shown that $E_0 \leq E_{\mathrm{P}}$!
  - there is no contradiction in the existence of two "minimums"
  - 1. $\hat{\mathbf{n}} \cdot \boldsymbol{B}_{\mathrm{P}}$ matches $\hat{\mathbf{n}} \cdot \boldsymbol{B}$ on all boundaries
  - 2. $\hat{\mathbf{n}} \cdot \boldsymbol{B}_0$ only matches $\hat{\mathbf{n}} \cdot \boldsymbol{B}$ on $z = 0$ and $z = L_z$
    - case 1. is a stronger constraint, for a specified $\boldsymbol{B}$
    - correspondingly the potential field energy in this case is higher

Summary

- Coronal magnetic fields power flares and CMEs
  - The NLFFF model is used to reconstruct the coronal field
    - with boundary values from vector magnetograms
- cfit is a Cartesian NLFFF code using the Grad-Rubin method
  - which may be used for modeling from solar data
  - or to investigate field configurations with analytic BCs
- For analytic bipolar fields with given B_z and different α
  - NLFFF solutions are found for a range of values of α
  - with energy which scales as α^2
  - up to an upper limit in α
    - but the origin of this limit is unclear
- The basic field decomposition used by cfit
  - illustrates an interesting subtlety in Thomson's theorem